In vivo wireless photonic photodynamic therapy

Akshaya Bansal[a,b], Fengyuan Yang[c], Tian Xi[c], Yong Zhang[a,b,1], and John S. Ho[b,c,d,1]

[a]Department of Biomedical Engineering, Faculty of Engineering, National University of Singapore, Singapore 117583, Singapore; [b]Biomedical Institute for Global Health Research and Technology, National University of Singapore, Singapore 117599, Singapore; [c]Department of Electrical and Computer Engineering, Faculty of Engineering, National University of Singapore, Singapore 117583, Singapore; and [d]Singapore Institute for Neurotechnology, National University of Singapore, Singapore 117456, Singapore

Edited by John A. Rogers, Northwestern University, Evanston, IL, and approved December 20, 2017 (received for review October 8, 2017)

An emerging class of targeted therapy relies on light as a spatially and temporally precise stimulus. Photodynamic therapy (PDT) is a clinical example in which optical illumination selectively activates light-sensitive drugs, termed photosensitizers, destroying malignant cells without the side effects associated with systemic treatments such as chemotherapy. Effective clinical application of PDT and other light-based therapies, however, is hindered by challenges in light delivery across biological tissue, which is optically opaque. To target deep regions, current clinical PDT uses optical fibers, but their incompatibility with chronic implantation allows only a single dose of light to be delivered per surgery. Here we report a wireless photonic approach to PDT using a miniaturized (30 mg, 15 mm^3) implantable device and wireless powering system for light delivery. We demonstrate the therapeutic efficacy of this approach by activating photosensitizers (chlorin e6) through thick (>3 cm) tissues inaccessible by direct illumination, and by delivering multiple controlled doses of light to suppress tumor growth in vivo in animal cancer models. This versatility in light delivery overcomes key clinical limitations in PDT, and may afford further opportunities for light-based therapies.

photodynamic therapy | wireless powering | bioelectronics | phototherapy

Since the early application of light to treat psoriasis (1), advances in understanding and engineering light–tissue interactions have enabled a class of targeted therapies with unmatched spatiotemporal resolution. Photodynamic therapy (PDT) is a clinical example in which light-sensitive drugs (photosensitizers) are selectively activated by light (2, 3), producing reactive oxygen species (ROS) which can be used to kill malignant cells; other emerging treatments include photothermal therapy (4) and photobiomodulation (5). Clinical application of PDT, however, has been hindered by the low penetration of light through biological tissue, which limits the therapeutic depth to less than a centimeter, even at near-infrared wavelengths (6–10). Currently, light delivery into deeper tissue regions relies on optical fibers inserted through surgery (11, 12) or endoscopy (13), but their incompatibility with long-term implantation allows only a single light dose to be delivered. This limitation in light delivery precludes the use of PDT for long-term therapy to suppress tumor recurrence or to tailor the dose to the tumor response.

Here we demonstrate a wireless photonic approach to PDT that enables on-demand light activation of photosensitizers deep in the body. We use an implantable photonic device and wireless powering system to deliver therapeutic doses of light into tissues inaccessible by direct illumination. The miniaturized (30 mg, 15 mm^3) dimensions of the device allows its direct implantation at the target site, where a specialized radio-frequency system wirelessly powers the device and monitors the light dosing rate. The light-delivery system integrates key advances over prior nontherapeutic systems (14–17) to enable practical PDT: (*i*) deep operation near organs at human size scales, (*ii*) multiwavelength light emission at radiant power levels optimized for photosensitizer activation, and (*iii*) wireless control of light emission for therapeutic dosimetry. We demonstrate wireless delivery of light deep in the body in situ by activating photosensitizers through thick (>3 cm) biological tissue and the efficacy of the light dose for PDT in vivo by inhibiting tumor growth in a murine cancer model.

Results

System Design. Fig. 1*A* illustrates the key steps in cancer PDT with the wireless device. First, the device is inserted near the target lesion. Because of its small dimensions, the device is compatible with minimally invasive implantation during standard clinical procedures such as incisional biopsy or during surgical tumor resection to combat tumor recurrence. Second, the photosensitizer—by itself harmless—is administered. Finally, the device is wirelessly powered, illuminating the tumor and resulting in the localized production of cytotoxic ROS that directly kill malignant cells, damage the tumor microvasculature, and/or stimulate the host immune response. By spatially and temporally controlling the light dose, the therapy can be tailored for maximum efficacy and minimum side effects.

Fig. 1 *B* and *C* and *SI Appendix*, Fig. S1 show the device and its schematic. The device consists of a 3D helical coil that extracts energy from the incident radio-frequency field and a microprinted circuit board (PCB) integrating the radio-frequency rectifier and two light-emitting diodes (LEDs). The LEDs were selected to match the emission spectrum to the absorption peaks of chlorin e6 (Ce6, 660 and 400 nm) (Fig. 1*D* and *SI Appendix*, Fig. S2), a clinically approved photosensitizer widely used for cancer treatment (18, 19), although the general configuration can be used with any photosensitizer with an overlapping activation spectrum. The helical coil and PCB are encapsulated in optically transparent and medical-grade silicone, resulting in a device that weighs 30 mg and is 15 mm^3 in volume. Silicone flaps were designed to control device orientation and for ease of fixation through sutures. The device emits light when wirelessly powered in a radio-frequency field with sufficient radiant power to fully illuminate a tumor volume about 5 mm in diameter (Fig. 1*E*).

Significance

The low penetration of light through tissue currently limits the therapeutic depth of photodynamic therapy (PDT) to less than a centimeter, even at near-infrared wavelengths. We report a wireless photonic approach to PDT in which miniaturized implantable devices deliver controlled doses of light by wireless powering through thick tissue. We demonstrate targeted cancer therapy with this approach by activating light-sensitive drugs deep in the body and suppressing tumor activity in vivo in animal models. The versatility in light delivery enabled by this approach extends the spatial and temporal precision of PDT to regions deep within the body.

Author contributions: A.B., F.Y., T.X., Y.Z., and J.S.H. designed research; A.B., F.Y., T.X., Y.Z., and J.S.H. performed research; A.B., F.Y., Y.Z., and J.S.H. analyzed data; and A.B., F.Y., Y.Z., and J.S.H. wrote the paper.

Conflict of interest statement: A provisional patent application has been filed based on the technology described in this work.

This article is a PNAS Direct Submission.

[1]To whom correspondence may be addressed. Email: biezy@nus.edu.sg or johnho@nus.edu.sg.

This article contains supporting information online at www.pnas.org/lookup/suppl/doi:10.1073/pnas.1717552115/-/DCSupplemental.

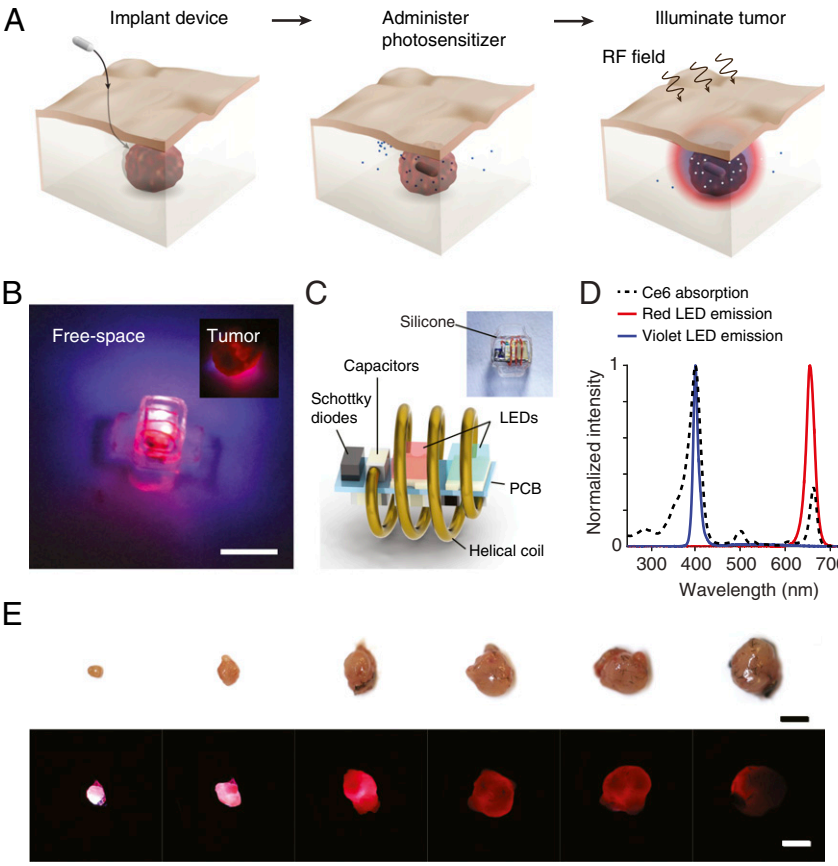

Fig. 1. Wireless photonic PDT. (*A*) Schematic of the therapy. The therapy consists of implantation of a wireless LED near the target region, administration of the photosensitizer, and wireless powering of the device. Light emitted by the device locally activates the photosensitizers and induces tumor damage. (*B*) Image of the wireless photonic device emitting light. (*Inset*) The device illuminating an explanted tumor. (Scale bar, 2 mm.) (*C*) Schematic of the device and individual electronic components. (*D*) Optical emission spectrum of the device from two LEDs. The emission wavelengths are centered at 400 nm (violet) and 660 nm (red), overlapping with the absorption peaks in the Ce6 spectrum. (*E*) Image panel of the penetration of light emitted by the device (radiant power, 1.3 mW) through tumors of increasing volume. (Scale bar, 5 mm.)

The encapsulation determines the biocompatibility of the device since the electronic components are not exposed to the physiological environment. Encapsulated devices remained functional over 180 d of submersion in phosphate-buffered solution and cell media at 37 °C (*SI Appendix*, Fig. S3). In addition, coincubation with cancer (MB49) and noncancer (HEK293T) model cells did not exhibit cytotoxicity as measured by calcein and propidium iodide fluorescence staining (20) (*SI Appendix*, Fig. S3).

Light transport simulations and experiments characterize the distribution of light around the device in tumor-like tissue in detail. Optical measurements within a synthetic tissue slab show that the irradiance contours approximate a sphere with center offset in the direction of emission at both wavelengths owing to light scattering (Fig. 2 *A* and *B* and *SI Appendix*, Fig. S4). The emission is directional, indicating control of the orientation of the LEDs is important, although optical scattering limits the spatial selectivity of the light delivery. Simulations estimate that at a total radiant power of 1.3 mW, the irradiance reaches 1 mW/cm^2 at a radius of 4 mm for red and 1.2 mm for violet light in the direction of maximum intensity, resulting in optical exposure of ∼2 J/cm^2 over a period of 30 min (Fig. 2 *C* and *D*), which is sufficient to activate most photosensitizers (21, 22). These estimates are consistent with the experiments in explanted tumor tissues (Fig. 1*E*), which show the penetration of light through about 5-mm thickness. For the selected emission wavelengths, the blood volume fraction of the tissue is important in determining the range of light delivery (*SI Appendix*, Fig. S5); the therapeutic volume depends on the type of tumor mass and may be greater for less-vascularized tumors. The wireless powering system is capable of achieving these levels of radiant power deep in tissue-like material. In the midfield configuration, the maximum radiant power that can be delivered by the device exceeds 1 mW at a 4-cm depth in water at a transmit power of 2 W (Fig. 2*F*). Prior studies using a phase-controlled transmitter show that exposure to the radio-frequency field results in a mild thermal effect (less than 3 °C) localized near the skin surface (23). The performance of the system meets the requirements for light delivery to tumors deep in the body and enables illumination of volumes up to ∼130 mm^3 (assuming a hemisphere volume of radius 4 mm), ∼8× the volume of the device.

A wireless dosimetry system (Fig. 2*E*) controls the light dose delivered to the target region. The system is based on the measurement of harmonic signals backscattered during wireless powering: As the device is powered near activation threshold, the nonlinearity of the LEDs results in an abrupt increase in the harmonic signal level, which is detected and used as an absolute reference for establishing the desired light-dosing rate (*SI Appendix*, Fig. S6). The backscattered harmonic signal also facilitates the placement of the transmitter on the body surface to optimize the transfer efficiency and avoid misalignment between transmitter and receiver (*SI Appendix*). The sensitivity of light delivery to variations in wireless powering can be further reduced by incorporating a clamping circuit to limit light emission beyond the target rate. Across a twofold increase or decrease in power level around the operating point

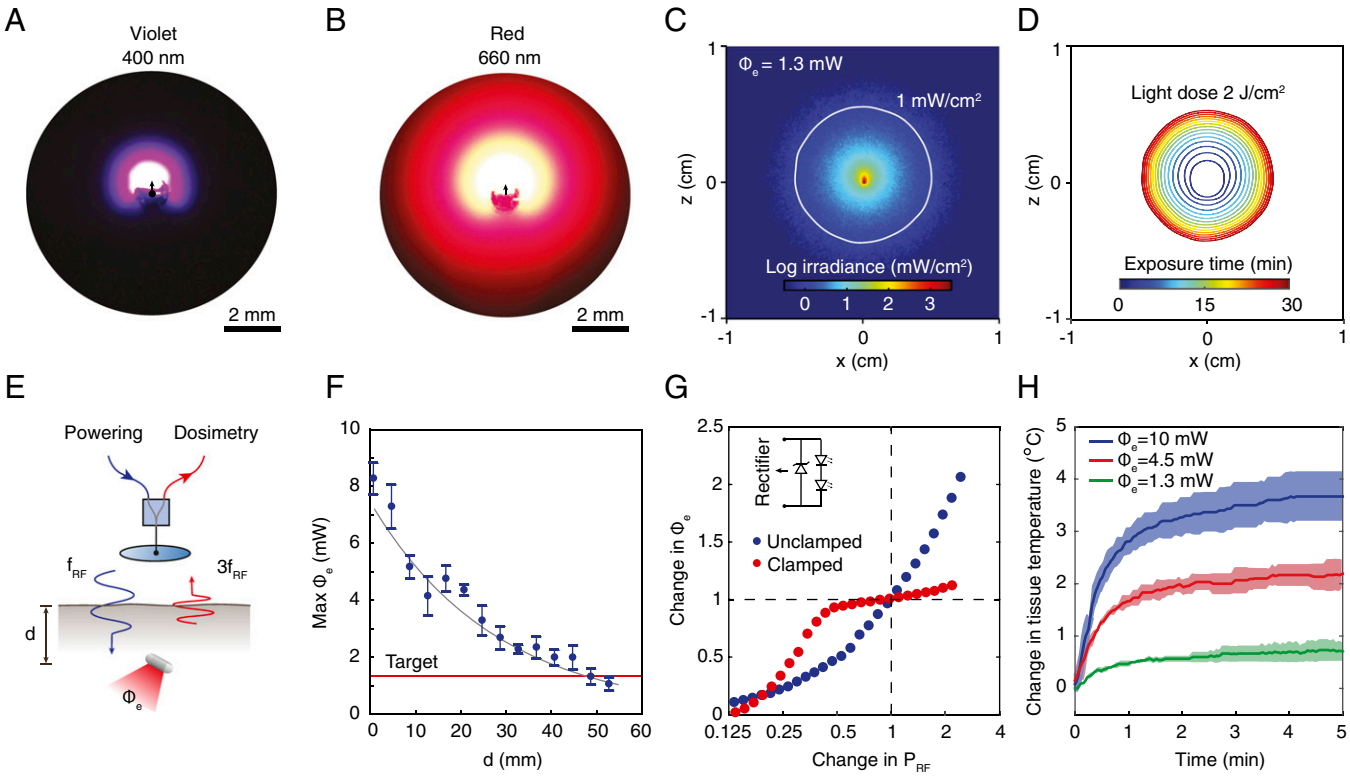

Fig. 2. Light distribution and wireless light delivery. (*A* and *B*) Image of the (*A*) violet and (*B*) red light distribution around the device in a synthetic tissue slab. (*C*) Numerical simulation of the optical irradiance around a device embedded in homogeneous tumor-like tissue, Φ_e, emitted radiant power, or equivalently, light-dosing rate. Solid white line shows 1-mW/cm^2 irradiance contour. (*D*) Light-dose contours (2 J/cm^2) from 1 to 30 min of exposure. (*E*) Schematic of the wireless light-delivery system. An external transmitter wirelessly powers the device at frequency f_{RF} and the backscattered third harmonic signal $3f_{RF}$ is measured to establish Φ_e. (*F*) Maximum radiant power Φ_e that can be delivered as a function of the depth of the device in tissue-simulating water. The device is powered in the midfield configuration with an output power P_{RF} of 2 W. (*G*) Change in Φ_e as a function of change in P_{RF} with and without a Zener clamp to regulate light emission. (*H*) In vivo local heating of tumor tissue under light exposure. Graphs show mean ± SD (n = 3 technical trials).

(radiant power, 1.3 mW), the circuit reduces the variation in light output from 70% to less than 10% (Fig. 2*G*). Thermal measurements show that the delivery of the light dose at the 1.3-mW rate limits the heat generated in tumor tissue to less than 1 °C over 2-min irradiation after which the temperature reaches steady state (Fig. 2*H*), which is well below thresholds for tissue damage.

In Vitro PDT. Photodynamic activity induced by the device deep in tissue was tested both in vitro and in situ. Dose–response curves of Ce6 in solution under LED illumination show ROS production rates increasing with Ce6 concentration (0–8 μM) and light dose, set by varying the exposure time (0, 20, and 40 min) and radiant power (1.3 and 4.5 mW) (*SI Appendix*, Figs. S7–S10). Direct LED illumination of zinc phthalocyanine and protoporphyrin IX, two other clinically used photosensitizers with an absorption peak near 660 nm, also resulted in comparable levels of ROS in vitro (*SI Appendix*, Fig. S11), indicating that the LED-mediated photodynamic effect is not specific to the choice of photosensitizer.

To illustrate that these devices could be powered through thick tissue at depths relevant to human scales, ROS production studies were conducted in an adult pig model. Fig. 3 *A*–*C* show computed tomography (CT) reconstructions of the radio-frequency transmitter and device implanted in the abdomen, with the transmitter placed on the skin and the device placed 5.1 cm deep, on the liver surface. Wireless light delivery by the device activated Ce6 and caused significant ROS production when powered through the thick intervening tissue (Fig. 3*D*) [$P < 0.0001$ between control (no Ce6) and test (solution containing 5 μM Ce6)].

Using Ce6-incubated murine bladder cancer cells, ROS production was further validated against red laser irradiation, the current clinical standard (24), in two configurations: (*i*) cells directly exposed to the radio-frequency/laser source, and (*ii*) cells placed under thick (3 cm) porcine tissue, simulating light delivery to deep tissue regions (Fig. 3 *E* and *F*). Wireless illumination with the device resulted in increased signal from a fluorogenic, cell-permeable ROS sensor (Image-iT live Green ROS), both in close proximity to the radio-frequency source and through thick tissue (Fig. 3*I*). In contrast, laser illumination (37.5 mW/cm^2, 4 J/cm^2) was effective only under direct irradiation: obstruction of the beam with thick tissue resulted in insignificant ROS-induced fluorescence. Controls consisting of light, radio-frequency field, or Ce6 exposure alone also did not result in significant ROS production (Fig. 3*J*). In all cases, significant cell death resulted from oxidative stress (Fig. 3*G*). Specifically, wireless light delivery resulted in nearly 80% cell kill in both configurations (P = 0.0027 direct and P = 0.0039 through thick tissue), whereas laser illumination obstructed by thick tissue did not result in a significant difference in cell viability (P = 0.178). Cell death could be attributed to apoptosis, a widely accepted mechanism for PDT-mediated cytotoxicity (Fig. 3*H*) (25, 26). These results demonstrate successful light-based targeting of malignant cells in regions inaccessible by direct laser illumination.

In Vivo PDT. We next demonstrated the efficacy of the light-delivery system for cancer PDT in C57BL/6 mice. The cancer model enables the therapeutic effect of the light dose to be tested in vivo, although the small size of the animals does not reproduce the depth of target region. The light dose was set to the same level (1.3 mW, 30 min) as used in the in vitro experiments. Devices were implanted in the interstitial space around a

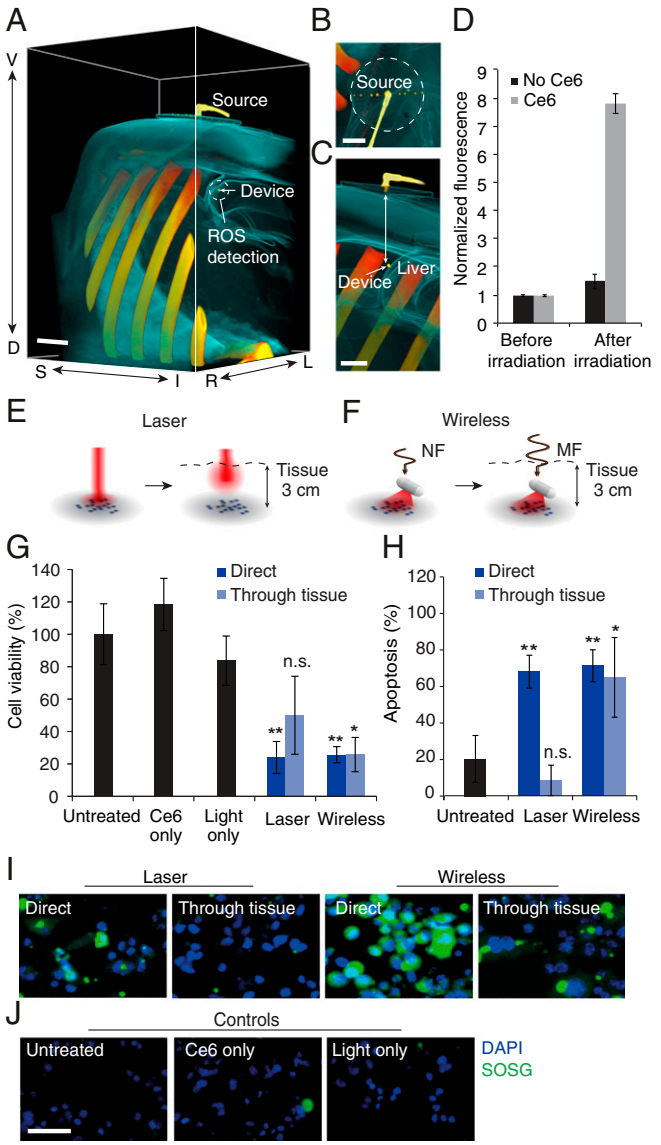

Fig. 3. Deep-tissue PDT of tumor cells. (*A–C*) Three-dimensional CT reconstruction of wireless light delivery in adult pig model showing (*A*) abdominal region, (*B*) radio-frequency transmitter, and (*C*) cross section. The depth of the device from the surface is 5.1 cm. (Scale bar, 2 cm.) (*D*) ROS production in Ce6 solution around the device. Values are mean ± SD ($n = 3$ per group). (*E* and *F*) Illustration of light-delivery configuration for irradiating MB49 cells using (*E*) laser and (*F*) device, with and without intervening thick porcine tissue. Near-field (NF) wireless powering is used at close proximity and midfield (MF) for thick tissue. (*G*) Change in cell viability (MTS assay) following 20 min of irradiation in the above light-delivery configurations. Groups include untreated cells, cells exposed to Ce6 alone, cells exposed to light alone, and cells incubated with Ce6 and exposed to light from a laser or the device with or without intervening tissue section. (*H*) Apoptosis index (TUNEL assay) including positive and negative controls from the assay. (*I* and *J*) Fluorescence images showing ROS production (green) in (*I*) cells treated following incubation with Ce6 and illumination in the two light-delivery configurations and (*J*) control cells left untreated or administrated light or Ce6 only. Blue: DAPI, green: SOSG. (Scale bar, 50 μm.) The light-dosing rate is 1.3 mW throughout. Graphs show mean ± SD ($n = 3$ per group). $^{**}P < 0.01$ and $^{*}P < 0.05$.

solid tumor (*SI Appendix*, Fig. S12) grown to 4–6 mm diameter from MB49 bladder cancer cells s.c. injected into the hind region. After a recovery period, PDT was performed by intratumoral injection of Ce6 followed 4 h later by wireless delivery of the light dose. Photosensitizers administered intratumorally have been shown to be retained in tumors for several hours, which is sufficient for the duration of the treatment (27). A second round of treatment was administered 7 d after the first, demonstrating ease of light delivery over long time scales. Control groups were left untreated; received Ce6 injections only; received sham devices only; or given light doses using functional devices without Ce6 injection.

Monitoring of the tumor volume as a function of time revealed suppression, and in some cases complete regression, of tumors in the treatment group compared with control groups (Fig. 4 *A–C*). Wireless delivery of light dose alone did not significantly affect tumor growth, indicating that the treatment efficacy was not due to the mild thermal effect of light and/or radio-frequency field exposure. Monitoring of tumor volume ended 13 d after first treatment, beyond which tumors in the majority of the mice from control groups either reached ethical size limits or were ulcerated. Across all groups, mice were otherwise healthy and did not show appreciable weight loss (Fig. 4*D*). Resection and histological examination (cryosectioning and TUNEL staining) of tumors revealed a significantly greater population of apoptotic cells in the treatment group compared with control groups, indicating that photodynamic activity is the likely mechanism for tumor destruction (Fig. 4*B*). Tumor volumes cleared by PDT at the prescribed light dose are consistent with light transport calculations and measurements (Fig. 2 *A* and *B*).

We compared the therapy to PDT by direct laser illumination, the current clinical standard, by histological examination of the tissue following a single round of treatment. Tumor-bearing mice were injected intratumorally with Ce6 and administered either the prior light dose using the wireless device or using a red laser (660 nm) collimated to a 5-mm diameter spot (*Materials and Methods*). In both cases, explanted tumor tissues showed comparable apoptosis (Fig. 4*E*), but tissues sampled from regions adjacent to the tumor did not show significant damage as assessed by TUNEL staining (Fig. 4*F*). Thermal measurements show that radio-frequency field exposure induces less than 2 °C increase in skin temperature after 4 min of operation (*SI Appendix*, Fig. S13) and was less than laser illumination (10). These results suggest that PDT by wireless light delivery does not result in increased damage to healthy tissues compared with current clinical standards.

We also characterized the in vivo immune response by implanting devices in the left flank of nontumor-bearing mice and evaluating the response 3 wk after implantation. Implanted animals did not exhibit a significant difference in systemic response compared with nonimplanted animals as measured by blood fibrinogen and C3 complement concentration (*SI Appendix*, Fig. S3 *D* and *E*) (28–30). Explantation of the device revealed a thin (<1 mm) fibrotic capsule around the device (*SI Appendix*, Fig. S3*C*). Histological sectioning and H&E staining of tissues surrounding the device did not reveal significant differences in morphology compared with control tissues from the right flank (*SI Appendix*, Fig. S3*C*). Although additional studies will be needed to assess long-term performance, the PDT results indicate that the performance is not degraded by the foreign body response over the duration of the study.

Discussion

We have demonstrated a wireless implantable photonic device that achieves therapeutic light delivery for cancer PDT. The operation of the device deep in the body is enabled by a radio-frequency system for wireless powering and monitoring of the light dose. As proof of concept, we wirelessly activated photosensitizers in situ in a porcine model of tissue and suppressed tumor activity in vivo in a murine cancer model by delivering light doses for PDT. The versatility of light delivery enabled by this approach overcomes the depth limitation of conventional PDT and extends its spatiotemporal precision to regions not directly accessible to light.

The implantation of the device will be a critical step in clinical applications. The device could be implanted during surgical resection of the tumor to perform PDT to suppress cancer

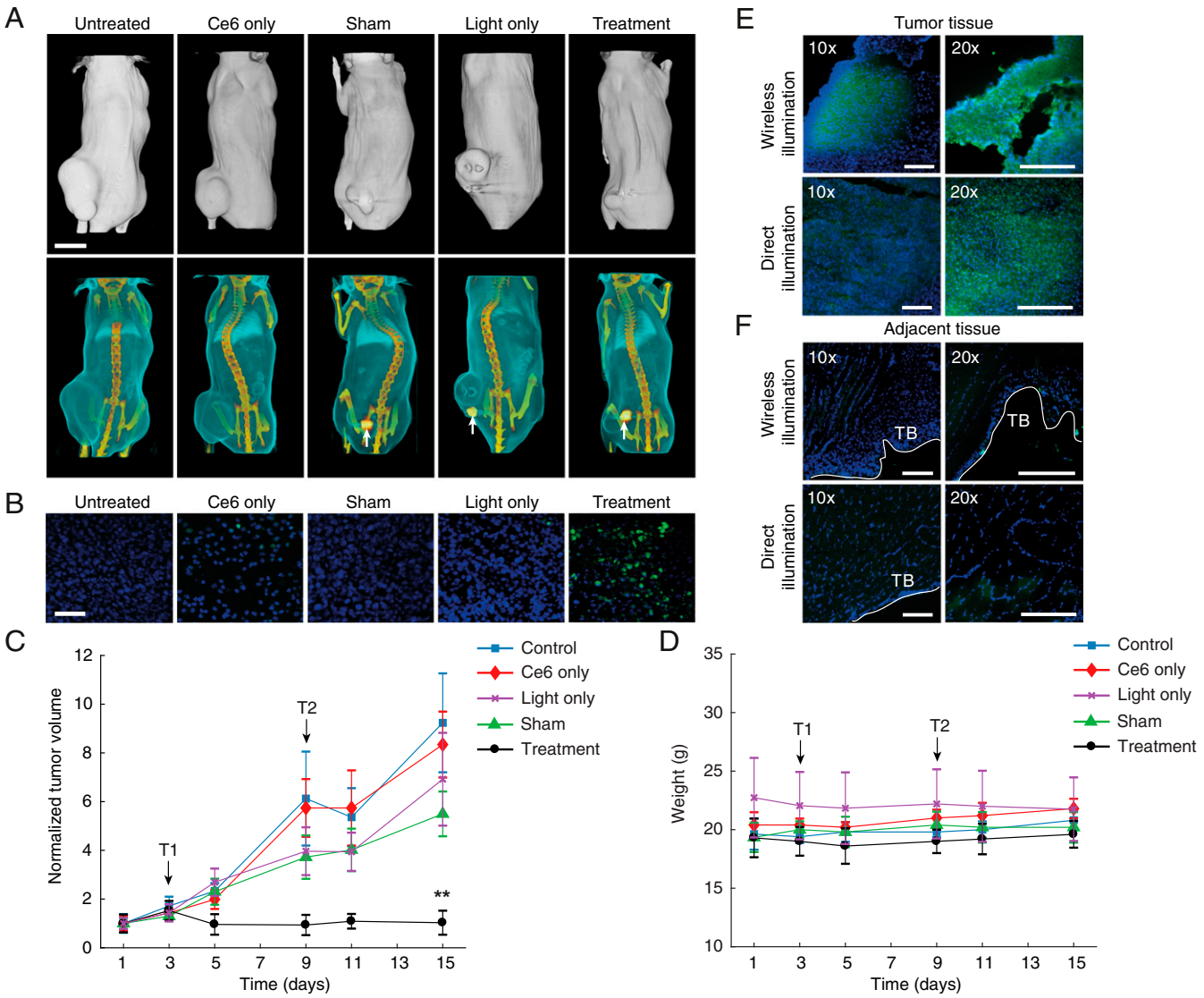

Fig. 4. In vivo PDT. (*A*) CT reconstructions of representative mice in each group 13 d after first treatment. White arrows show implant position. (Scale bar, 1 cm.) (*B*) Stained tumor tissue sections from each group. DAPI (blue) shows cell nuclei and TUNEL (green) staining indicates apoptosis. (Scale bar, 50 μm.) (*C*) Normalized tumor volume as a function of time during the monitoring period. Treatments are administered on day 3 (T1) and day 9 (T2) with a light dose of 1.3 mW over 30 min. (*D*) Body weight over the treatment period. (*E*) Stained sections of tumor tissue following a single round of treatment using either wireless light delivery (wireless illumination) or laser light (660 nm) delivery (direct illumination). (*F*) Stained sections of healthy tissues adjacent to the tumor. T.B., tissue boundary. (Scale bar, 200 μm.) Graphs show mean ± SD ($n = 5$ per group). $^{**}P < 0.01$.

recurrence. Because of its small dimensions, the device could also be designed to be compatible with minimally invasive implantation techniques such as needle injection, potentially during biopsy of the target region. Long-term implantation of the device will also require hermetic encapsulation compatible with light delivery and wireless powering; in this context, silicone and glass encapsulations have been extensively developed by the medical device industry and can achieve functional lifetimes of many years. Because of the contactless nature of light delivery, the system could potentially be more robust to fibrosis compared with conventional modalities such as electrostimulation or drug delivery. Due to optical scattering and powering constraints, the therapeutic volume of light delivery for the current system is about 1 cm in diameter, which limits its efficacy for large tumor masses. Greater coverage could be obtained by using photosensitizers or upconversion nanoparticles activated at near-infrared wavelengths (10), or by distributing multiple LEDs over the treatment region.

The PDT protocol could be further optimized to enhance the treatment efficacy. First, targeting the photosensitizer for uptake into tumor cells could increase the selectivity of the treatment. Carrier-mediated drug delivery has been extensively studied for PDT (8), and could be combined with our light-delivery system to achieve cellular-level specificity to minimize damage to healthy tissues exposed to light. Second, the PDT regimen could be fractionated or repeated over longer time scales to improve treatment outcomes. Fractionated dosing of photosensitizers, for example, has been used to enhance targeting of both vasculature and tumor-cell compartments (31), and pulsed-light dosing to circumvent photosensitizer saturation or oxygen depletion (32). Finally, because the mechanisms of PDT are distinct from conventional chemotherapeutics, our approach could also be combined with cancer drugs to overcome drug resistance and stimulate an antitumor immune response (33–36).

Potential clinical targets for which our approach could provide advantages include hepatocellular carcinomas or glioblastomas, where PDT currently provides promising outcomes compared with conventional treatment (37, 38) but has been hindered by the inaccessibility of the target region to light. The versatility of light delivery allows light doses to be delivered over long time scales in a programmable and repeatable manner, and could potentially enable the therapies to be tailored in real time. Beyond PDT, the technology can be adapted for use in light-based therapies (20) such as photothermal therapy, photocontrolled delivery of drugs, or photobiomodulation, and integrated with sensors to monitor the treatment response in real-time. Translating these capabilities to the clinic will provide new opportunities to shine light on human disease.

Materials and Methods

Wireless Powering System. Wireless powering used a transmitter driven by a radio-frequency signal between 1 and 1.5 GHz. Transmitters were designed for operation both in the electromagnetic near-field (close range, <1-cm distance) and midfield (deep in tissue, >1-cm) ranges. Wireless powering for a prescribed light-dosing rate was established in two steps (*i*): while holding the transmit power constant, the transmitter position was adjusted until the measured harmonic backscatter was maximized (compensating for potential misalignment between the transmitter and receiver) (*ii*); while holding the transmitter position constant, the transmit power was tuned such that the light emission was set to the desired level using the dosimetry system. Detailed methods may be found in *SI Appendix, Materials and Methods*.

In Vivo PDT in Murine Model of Bladder Carcinoma. Studies conformed to the Guide for the Care and Use of Laboratory Animals published by the National Institutes of Health, USA and protocol approved by the Institutional Animal Care and Use Committee, National University of Singapore. Tumors were induced in C57BL/6 mice by s.c. implanting 2×10^6 to 3×10^6 MB49 bladder cancer cells in the lower flank. Two- to three weeks after inoculation of tumor cells, mice were randomly divided into five groups ($n = 5$ per group) (*i*) control untreated; (*ii*) administered with Ce6, but not given a device; (*iii*) implanted with sham (nonfunctional) devices; (*iv*) implanted with functional devices, but not administered Ce6; and (*v*) treatment group given both Ce6 and a functional device. Devices were implanted in groups 3, 4, and 5 and treatment commenced 1 wk after implantation, during which tumors across all groups were ∼4–6 mm in diameter. At the start of treatment, groups 2 and 5 were injected intratumorally with 10 mg/kg of Ce6. Groups 4 and 5, implanted with functional devices, were anesthetized 4 h after injection, and the tumor illuminated wirelessly for 30 min per mouse. A second round of treatment was administered 7 d after following the same procedures as the first for each group. The study ended 1 wk after the second round of treatment due to the need to euthanize mice in groups where tumors had reached the ethical limit. Detailed methods may be found in *SI Appendix, Materials and Methods*.

ACKNOWLEDGMENTS. We thank Ms. Niagara Muhammed Idris for her assistance in device implantation surgery and advice on experimental design. This work was supported by grants from the Ministry of Education (MOE2016-T3-1-004), National Research Foundation (NRF-NRFF2017-07), and the Biomedical Institute of Global Health Research and Technology.

1. Fritsch C, Goerz G, Ruzicka T (1998) Photodynamic therapy in dermatology. *Arch Dermatol* 134:207–214.
2. Dolmans DE, Fukumura D, Jain RK (2003) Photodynamic therapy for cancer. *Nat Rev Cancer* 3:380–387.
3. Brown SB, Brown EA, Walker I (2004) The present and future role of photodynamic therapy in cancer treatment. *Lancet Oncol* 5:497–508.
4. Jin CS, Lovell JF, Chen J, Zheng G (2013) Ablation of hypoxic tumors with dose-equivalent photothermal, but not photodynamic, therapy using a nanostructured porphyrin assembly. *ACS Nano* 7:2541–2550.
5. Chung H, et al. (2012) The nuts and bolts of low-level laser (light) therapy. *Ann Biomed Eng* 40:516–533.
6. Wilson BC, Patterson MS (2008) The physics, biophysics and technology of photodynamic therapy. *Phys Med Biol* 53:R61–R109.
7. Detty MR, Gibson SL, Wagner SJ (2004) Current clinical and preclinical photosensitizers for use in photodynamic therapy. *J Med Chem* 47:3897–3915.
8. Chatterjee DK, Fong LS, Zhang Y (2008) Nanoparticles in photodynamic therapy: An emerging paradigm. *Adv Drug Deliv Rev* 60:1627–1637.
9. Zhu TC, Finlay JC (2008) The role of photodynamic therapy (PDT) physics. *Med Phys* 35: 3127–3136.
10. Idris NM, et al. (2012) In vivo photodynamic therapy using upconversion nanoparticles as remote-controlled nanotransducers. *Nat Med* 18:1580–1585.
11. Brancaleon L, Moseley H (2002) Laser and non-laser light sources for photodynamic therapy. *Lasers Med Sci* 17:173–186.
12. Mang TS (2004) Lasers and light sources for PDT: Past, present and future. *Photodiagn Photodyn Ther* 1:43–48.
13. Yoon I, Li JZ, Shim YK (2013) Advance in photosensitizers and light delivery for photodynamic therapy. *Clin Endosc* 46:7–23.
14. Kim TI, et al. (2013) Injectable, cellular-scale optoelectronics with applications for wireless optogenetics. *Science* 340:211–216.
15. Park SI, et al. (2015) Soft, stretchable, fully implantable miniaturized optoelectronic systems for wireless optogenetics. *Nat Biotechnol* 33:1280–1286.
16. Montgomery KL, et al. (2015) Wirelessly powered, fully internal optogenetics for brain, spinal and peripheral circuits in mice. *Nat Methods* 12:969–974.
17. Shao J, et al. (2017) Smartphone-controlled optogenetically engineered cells enable semiautomatic glucose homeostasis in diabetic mice. *Sci Transl Med* 9:eaal2298.
18. Yu H, Li J, Wu D, Qiu Z, Zhang Y (2010) Chemistry and biological applications of photo-labile organic molecules. *Chem Soc Rev* 39:464–473.
19. Huang P, et al. (2011) Folic acid-conjugated graphene oxide loaded with photosensitizers for targeting photodynamic therapy. *Theranostics* 1:240–250.
20. Kim S-J, et al. (2012) Evaluation of the biocompatibility of a coating material for an implantable bladder volume sensor. *Kaohsiung J Med Sci* 28:123–129.
21. Yun SH, Kwok SJ (2017) Light in diagnosis, therapy and surgery. *Nat Biomed Eng* 1: 0008.
22. Bachor R, Shea CR, Gillies R, Hasan T (1991) Photosensitized destruction of human bladder carcinoma cells treated with chlorin e6-conjugated microspheres. *Proc Natl Acad Sci USA* 88:1580–1584.
23. Agrawal DR, et al. (2017) Conformal phased surfaces for wireless powering of bioelectronic microdevices. *Nat Biomed Eng* 1:0043.
24. Luo W, Liu R-S, Zhu J-G, Li Y-C, Liu H-C (2015) Subcellular location and photodynamic therapeutic effect of chlorin e6 in the human tongue squamous cell cancer Tca8113 cell line. *Oncol Lett* 9:551–556.
25. Allison RR, et al. (2004) Photosensitizers in clinical PDT. *Photodiagn Photodyn Ther* 1: 27–42.
26. Oleinick NL, Morris RL, Belichenko I (2002) The role of apoptosis in response to photodynamic therapy: What, where, why, and how. *Photochem Photobiol Sci* 1: 1–21.
27. Zhang N, et al. (2016) Multitriggered tumor-responsive drug delivery vehicles based on protein and polypeptide coassembly for enhanced photodynamic tumor ablation. *Small* 12:5936–5943.
28. Bélanger MC, Marois Y (2001) Hemocompatibility, biocompatibility, inflammatory and in vivo studies of primary reference materials low-density polyethylene and polydimethylsiloxane: A review. *J Biomed Mater Res* 58:467–477.
29. Defrère S, et al. (2011) In vivo biocompatibility of three potential intraperitoneal implants. *Macromol Biosci* 11:1336–1345.
30. Lucky SS, et al. (2016) In vivo biocompatibility, biodistribution and therapeutic efficiency of titania coated upconversion nanoparticles for photodynamic therapy of solid oral cancers. *Theranostics* 6:1844–1865.
31. Dolmans DE, et al. (2002) Targeting tumor vasculature and cancer cells in orthotopic breast tumor by fractionated photosensitizer dosing photodynamic therapy. *Cancer Res* 62:4289–4294.
32. Sterenborg HJ, van Gemert MJ (1996) Photodynamic therapy with pulsed light sources: A theoretical analysis. *Phys Med Biol* 41:835–849.
33. Robertson CA, Evans DH, Abrahamse H (2009) Photodynamic therapy (PDT): A short review on cellular mechanisms and cancer research applications for PDT. *J Photochem Photobiol B* 96:1–8.
34. Castano AP, Mroz P, Hamblin MR (2006) Photodynamic therapy and anti-tumour immunity. *Nat Rev Cancer* 6:535–545.
35. Mitsunaga M, et al. (2011) Cancer cell-selective in vivo near infrared photoimmunotherapy targeting specific membrane molecules. *Nat Med* 17:1685–1691.
36. He C, et al. (2016) Core-shell nanoscale coordination polymers combine chemotherapy and photodynamic therapy to potentiate checkpoint blockade cancer immunotherapy. *Nat Commun* 7:12499.
37. Bahng S, et al. (2013) Photodynamic therapy for bile duct invasion of hepatocellular carcinoma. *Photochem Photobiol Sci* 12:439–445.
38. Muller PJ, Wilson BC (2006) Photodynamic therapy of brain tumors–A work in progress. *Lasers Surg Med* 38:384–389.